The remarkable orientation and concentration dependences of the electromechanical properties of $0.67Pb(Mg_{1/3}Nb_{2/3})O_3$–$0.33PbTiO_3$ single crystals

2004 J. Phys.: Condens. Matter 16 2115

(http://iopscience.iop.org/0953-8984/16/12/021)

INSTITUTE OF PHYSICS PUBLISHING JOURNAL OF PHYSICS: CONDENSED MATTER

J. Phys.: Condens. Matter **16** (2004) 2115–2128 PII: S0953-8984(04)69745-1

The remarkable orientation and concentration dependences of the electromechanical properties of $0.67Pb(Mg_{1/3}Nb_{2/3})O_3$–$0.33PbTiO_3$ single crystals

V Yu Topolov

Forschungszentrum Karlsruhe GmbH in der Helmholtz-Gemeinschaft,
Institut für Materialforschung II, Postfach 36 40, D-76021 Karlsruhe, Germany

E-mail: Vitali-Yu.Topolov@imf.fzk.de

Received 30 September 2003
Published 12 March 2004
Online at stacks.iop.org/JPhysCM/16/2115 (DOI: 10.1088/0953-8984/16/12/021)

Abstract

The present paper is devoted to evaluations of electromechanical constants of single-domain and multidomain relaxor-ferroelectric $0.67Pb(Mg_{1/3}Nb_{2/3})O_3$–$0.33PbTiO_3$ single crystals near the morphotropic phase boundary. For the rhombohedral single crystal ($3m$ class), piezoelectric coefficients and electromechanical coupling factors are calculated as functions of Euler angles. Features of orientation dependences of the piezoelectric coefficients and electromechanical coupling factors are first formulated and analysed. Two variants of concentration dependences of effective piezoelectric strain coefficients and electromechanical coupling factors are also first calculated, and the features of the piezoelectric activity of multidomain $0.67Pb(Mg_{1/3}Nb_{2/3})O_3$–$0.33PbTiO_3$ single crystals are discussed.

(Some figures in this article are in colour only in the electronic version)

1. Introduction

The problem of the dependence of physical properties of ferroelectric single crystals (SCs) on the orientation of their crystallographic axes [1–7] or on different domain types in multidomain (twinned) states [8–11, 3] has attracted considerable attention for the past three to four decades. In recent years, efforts of many researchers have been focused on the study of relaxor-ferroelectric perovskite-type solid solutions, such as $(1-x)Pb(Zn_{1/3}Nb_{2/3})O_3$–$xPbTiO_3$ (PZN–xPT) and $(1-x)Pb(Mg_{1/3}Nb_{2/3})O_3$–$xPbTiO_3$ (PMN–xPT), near the morphotropic phase boundary. Various experimental works on these compositions [12–14] indicate that a coexistence of morphotropic ferroelectric phases and complicated domain or twin structures is observed at room temperature. After poling the SC samples in the $[001]_c$ direction with respect to the perovskite or pseudocubic crystallographic axes, the rhombohedral ($3m$) phase is characterized by the very large

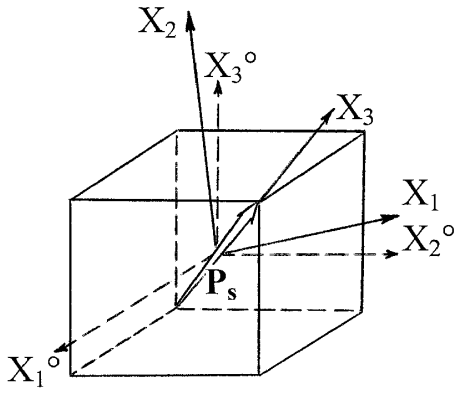

Figure 1. Orientation of the domain with respect to the principal OX_j and perovskite OX_j° axes. $\mathbf{P_s}$ is the spontaneous polarization vector.

piezoelectric strain coefficient d_{33} (over 2000 pC N^{-1}), electromechanical coupling factor k_{33} (over 90%) and large high-field strain (over 1%) [2, 6, 7, 15–18]. These and other performances of the above-mentioned relaxor-based SCs are of value for various modern applications, e.g., as electromechanical transducers, piezoelectric actuators, active elements of acoustic devices, highly effective components of piezoactive composites, etc. In the multidomain states, the macroscopic symmetry is reduced to $4mm$, $mm2$, or even lower [3], and the significant piezoelectric effect is often associated with so-called 'engineered domain structure' [2, 15, 16, 19]. Such structures and changes in them under external electric or mechanical fields [13, 14, 19–21] stimulate new studies in physics of ferroelectric phenomena, solid state physics, crystallography, physics of advanced materials, and physics of heterogeneous media.

In recent work, complete sets of electromechanical (i.e., piezoelectric, dielectric, and elastic) constants have been measured on multidomain or domain-engineered PZN–0.045PT [16, 22], PZN–0.08PT [22], PZN–0.09PT [23], PMN–0.30PT [24], PMN–0.33 PT [15], and PMN–0.38PT [25] SC samples poled in the $[001]_c$ direction. As for the single-domain SCs, their electromechanical constants have been first measured [26] on PMN–0.33PT samples with the rhombohedral $3m$ structure under the electric field bias $\mathbf{E} \parallel [001]_c$. Based on these experimental data, the piezoelectric coefficients d_{3j} ($j = 1, 3$) [4, 5], the dielectric constant ε_{33}^{T} of the stress-free sample [4], and the electromechanical coupling factor k_{33} [4] have been calculated along arbitrary directions. Other types of piezoelectric coefficient and related parameters have not yet been analysed in terms of the dependence on the orientation of the single-domain crystallographic axes or on the volume concentration of different domain types of the studied relaxor-based SCs. In this connection, the present work is aimed at the study and generalization of features of the orientation and concentration dependences of the electromechanical properties of PMN–0.33PT single- and multidomain SCs.

2. Orientation dependences of electromechanical properties in the single-domain state

In this section we show how the piezoelectric effect depends on the orientation of the crystallographic axes of the rhombohedral single-domain PMN–0.33PT SC. The spontaneous polarization vector $\mathbf{P_s}$ of this SC is assumed to be parallel to the $[001]_r$ direction (figure 1) in

Table 1. Room-temperature elastic compliances s^{E}_{ab} (in 10^{-12} Pa^{-1}), piezoelectric coefficients d_{ij} (in pC N^{-1}) and dielectric constants $\varepsilon^{\mathrm{T}}_{pp}/\varepsilon_0$ in the 3m phase of single-domain 0.67Pb($Mg_{1/3}Nb_{2/3}$)O_3–0.33$PbTiO_3$ crystals. (Note. 1. Electromechanical constants were calculated from results of measurements [26] and written in the principal crystallographic axes. 2. Values in parentheses were taken from the recent paper [4] for comparison.)

s^{E}_{11}	s^{E}_{12}	s^{E}_{13}	s^{E}_{14}	s^{E}_{33}	s^{E}_{44}	s^{E}_{66}	d_{15}	d_{22}	d_{31}	d_{33}	$\varepsilon^{\mathrm{T}}_{11}/\varepsilon_0$	$\varepsilon^{\mathrm{T}}_{33}/\varepsilon_0$
62.16	−53.85	−5.58	−166.24	13.34	510.98	232.02	4100	1340	−90	190	3950	640
(62.2)	(−53.8)	(−5.6)	(−166.2)	(13.3)	(511.0)	(232.0)						

the principal axes $(X_1X_2X_3)$ or to the $[111]_{\mathrm{c}}$ direction in the perovskite axes[1]. The arbitrary SC orientation caused by a transformation of the coordinate axes $(X_1X_2X_3) \rightarrow (X'_1X'_2X'_3)$ is described in terms of Euler angles φ, ψ, and θ [27]. The dielectric, piezoelectric, and elastic constants of the SC (table 1) can be written in the coordinate system $(X'_1X'_2X'_3)$ as components of tensors of the second, third, and fourth ranks, respectively, in the form

$$\varepsilon'^{\mathrm{T}}_{mn} = \alpha_{mp}\alpha_{nq}\varepsilon^{\mathrm{T}}_{pq}, \qquad d'_{efg} = \alpha_{ej}\alpha_{fk}\alpha_{gl}\,d_{jkl} \qquad \text{and} \qquad s'^{\mathrm{E}}_{rtuv} = \alpha_{ra}\alpha_{tb}\alpha_{uc}\alpha_{vd}s^{\mathrm{E}}_{abcd}. \quad (1)$$

In equations (1), α_{mp} are elements of the rotation matrix

$$\|\alpha\| = \begin{pmatrix} \cos\psi\cos\varphi - \sin\psi\cos\theta\sin\varphi & \cos\psi\sin\varphi + \sin\psi\cos\theta\cos\varphi & \sin\psi\sin\theta \\ -\sin\psi\cos\varphi - \cos\psi\cos\theta\sin\varphi & -\sin\psi\sin\varphi + \cos\psi\cos\theta\cos\varphi & \cos\psi\sin\theta \\ \sin\theta\sin\varphi & -\sin\theta\cos\varphi & \cos\theta \end{pmatrix}$$

that depends on the above-mentioned Euler angles [27]. After this transformation we introduce the conventional two-index form [27, 28] of notation of electromechanical constants; the analogous form is used, for example, in table 1.

The remaining types of piezoelectric coefficient in the coordinate system $(X'_1X'_2X'_3)$ are determined [27, 28] from the matrix equations $\|e'\| = \|d'\|\|s'^{\mathrm{E}}\|^{-1}$, $\|g'\| = \|\varepsilon'^{\mathrm{T}}\|^{-1}\|d'\|$ and $\|h'\| = \|\varepsilon'^{S}\|^{-1}\|e'\|$ where dielectric constants of the stress-free $\varepsilon'^{\mathrm{T}}_{lm}$ and clamped ε'^{S}_{lm} samples are interrelated by an equation $\varepsilon'^{\mathrm{T}}_{lm} - \varepsilon'^{S}_{lm} = e'_{lt}d'_{mt}$. Along with the orientation dependence of the piezoelectric coefficients $d'_{3j}(\varphi, \psi, \theta)$, $e'_{3j}(\varphi, \psi, \theta)$, $g'_{3j}(\varphi, \psi, \theta)$, and $h'_{3j}(\varphi, \psi, \theta)$, which describe the response related to the poling axis, we consider the electromechanical coupling factors $k'_{3j}(\varphi, \psi, \theta) = d'_{3j}(\varepsilon'^{\mathrm{T}}_{33}s'^{\mathrm{E}}_{jj})^{-1/2}$, where $j = 1, 2, 3$. The k'_{3j} factors are usually introduced for elongated SC bars of any direction and therefore often called 'length coupling factors'.

Starting from the principal crystallographic axes of the single domain (i.e. $\varphi = \psi = \theta = 0$), we calculated the orientation dependences of some piezoelectric coefficients (figures 2 and 3) and electromechanical coupling factors (figure 4) of the PMN–0.33PT SC. The main features of the calculated orientation dependences of the electromechanical properties of the single-domain rhombohedral SC are listed below.

Firstly, all the constants x'_{33}, where $x = d, e, g, h, k, s^{\mathrm{E}}, \varepsilon^{\mathrm{T}}$, are independent of the angle φ. Secondly, the following two variants of periodicity on the ψ angle have been established:

(i) for all the electromechanical constants x'_{3j} with $j = 1, 2$, equalities

$$x'_{31}(\varphi, \psi, \theta) = x'_{32}(\varphi, \psi + 90^\circ, \theta) \qquad \text{and} \qquad x'_{32}(\varphi, \psi, \theta) = x'_{31}(\varphi, \psi + 90^\circ, \theta) \quad (2)$$

hold true, whereas

[1] Interconnections between these directions and orientations of the crystallographic axes were considered, e.g., in papers [3, 5, 6].

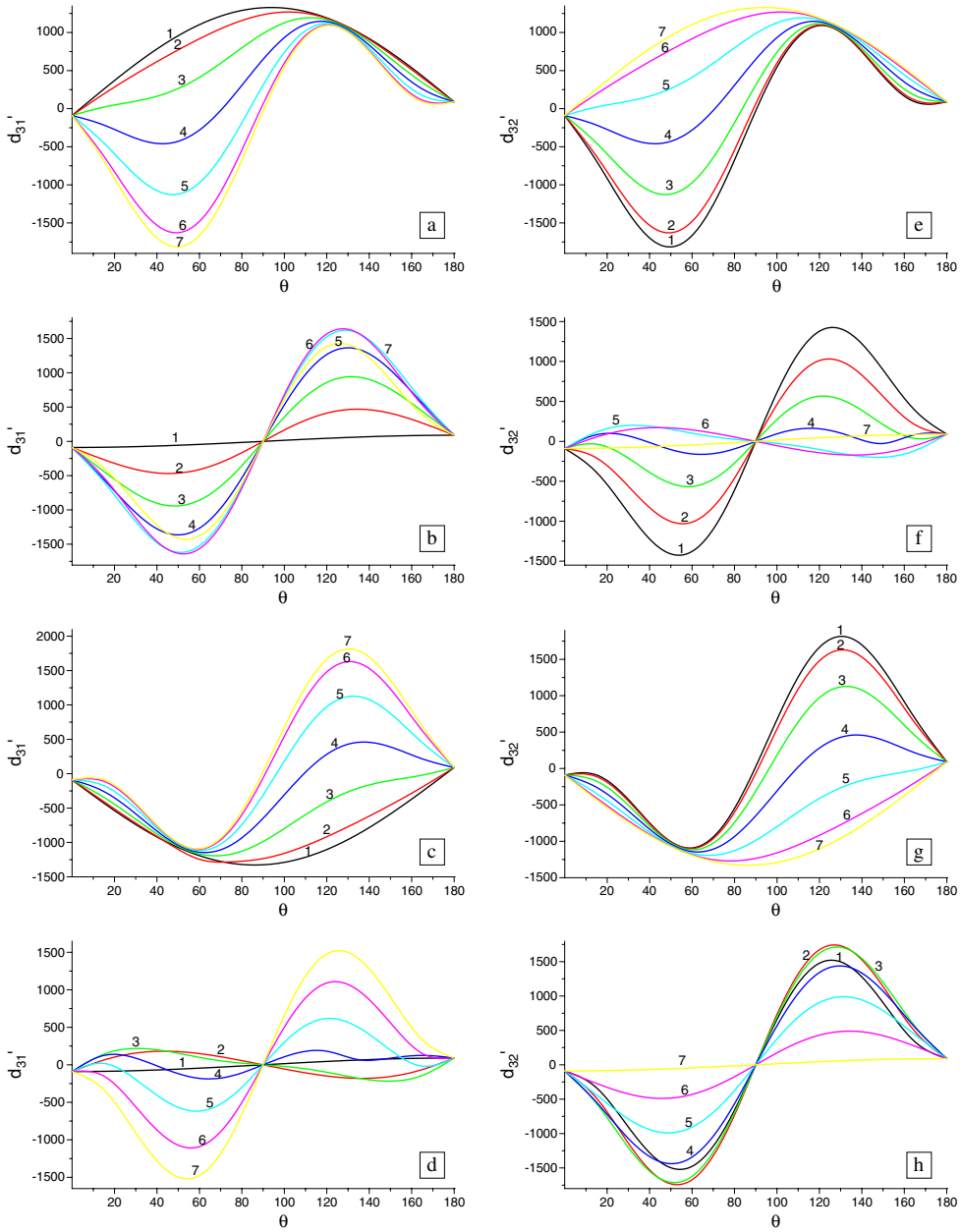

Figure 2. Piezoelectric coefficients $d'_{3j}(\varphi, \psi, \theta)$ (d'_{3j} in pC N^{-1}; φ, ψ, and θ in degrees) calculated for the single-domain PMN–0.33PT SC: (a) $j = 1$, $\varphi = 120°r$; (b) $j = 1$, $\varphi = 30° + 120°r$; (c) $j = 1$, $\varphi = 60° + 120°r$; (d) $j = 1$, $\varphi = 90° + 120°r$; (e) $j = 2$, $\varphi = 120°r$; (f) $j = 2$, $\varphi = 30° + 120°r$; (g) $j = 2$, $\varphi = 60° + 120°r$; (h) $j = 2$, $\varphi = 90° + 120°r$; (i) $j = 3$, no dependence on ψ. In graphs (a)–(h), curves 1, 2, 3, 4, 5, 6, and 7 were calculated for $\psi = 0°$, 15°, 30°, 45°, 60°, 75°, and 90°, respectively, and $r = 0$, 1, 2, and 3.

(ii) for all the electromechanical constants x'_{33}, no changes in subscripts are observed, and this circumstance results in an equality

$$x'_{33}(\varphi, \psi, \theta) = x'_{33}(\varphi, \psi + 90°, \theta). \tag{3}$$

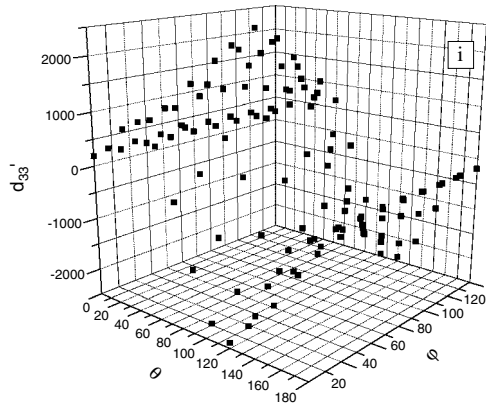

Figure 2. (Continued.)

Thirdly, for all the above-mentioned $x'_{3j}(\varphi, \psi, \theta)$ dependences, periodicity on the φ angle is associated with the presence of the threefold axis in the $3m$ class:

$$x'_{3j}(\varphi, \psi, \theta) = x'_{3j}(\varphi + 120^\circ, \psi, \theta) \tag{4}$$

where $j = 1, 2, 3$.

In addition, the following features of the $d'_{3j}(\varphi, \psi, \theta)$ dependences have been first revealed in this study:

(i) at $\theta = 90^\circ$, independently of the φ and ψ angles, the sum of the piezoelectric coefficients (i.e., the analogue of the hydrostatic piezoelectric coefficient of the poled ferroelectric ceramic) is given by

$$d'_{31}(\varphi, \psi, 90^\circ) + d'_{32}(\varphi, \psi, 90^\circ) + d'_{33}(\varphi, \psi, 90^\circ) = 0; \tag{5}$$

(ii) at $\varphi = 0$, $\psi = 45^\circ + 90^\circ r$, and independently of the θ angle, an equality

$$d'_{31}(0, \psi, \theta) = d'_{32}(0, \psi, \theta) \tag{6}$$

is realized;

(iii) at $\varphi > 0$, $\psi = 45^\circ + 90^\circ r$, and $\theta = 90^\circ$, a similar equality

$$d'_{31}(\varphi, \psi, 90^\circ) = d'_{32}(\varphi, \psi, 90^\circ) \tag{7}$$

holds true; and

(iv) at $\varphi = 30^\circ + 60^\circ r$, $\theta = 90^\circ$, and independently of the ψ angle, a specific case of equation (5) is given by

$$d'_{31}(\varphi, \psi, 90^\circ) = d'_{32}(\varphi, \psi, 90^\circ) = d'_{33}(\varphi, \psi, 90^\circ) = 0. \tag{8}$$

In equations (6) and (7), values $r = 1, 2, 3$ are assumed; equation (8) is written for $r = 1, 2, 3, 4, 5$.

As follows from equations (2)–(4) and (6)–(8) on periodic orientation behaviour of $x'_{3j}(\varphi, \psi, \theta)$, it is enough to calculate x'_{3j} in ranges of Euler angles

$$0 \leqslant \varphi \leqslant 120^\circ, \qquad 0 \leqslant \psi \leqslant 90^\circ \qquad \text{and} \qquad 0 \leqslant \theta \leqslant 180^\circ. \tag{9}$$

For all the angles that do not obey inequalities (9), relations (2)–(4) are to be used.

The above-mentioned elements of periodicity of the orientation dependence $x'_{3j}(\varphi, \psi, \theta)$ stem from features of the crystal structure of the polar $3m$ class and should be taken

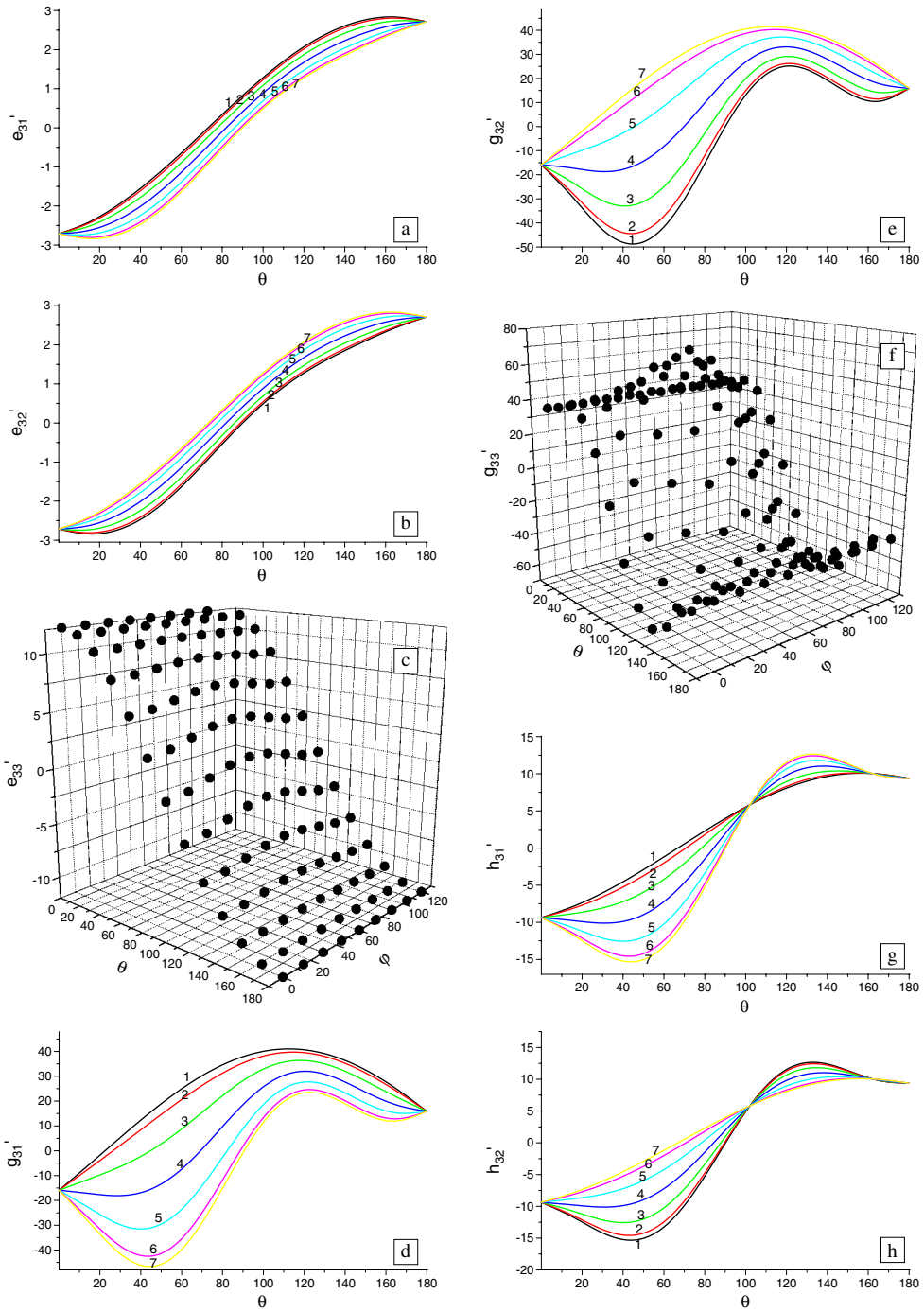

Figure 3. Piezoelectric coefficients $e'_{3j}(\varphi, \psi, \theta)$ (e'_{3j} in C m^{-2}; φ, ψ, and θ in degrees; graphs (a)–(c)), $g'_{3j}(\varphi, \psi, \theta)$ (g'_{3j} in mV m N^{-1}; φ, ψ, and θ in degrees; graphs (d)–(f)) and $h'_{3j}(\varphi, \psi, \theta)$ (h'_{3j} in 10^8 V m; φ, ψ, and θ in degrees; graphs (g)–(i)) which were calculated for the single-domain PMN–0.33PT SC: (a), (d), (g) $j = 1$, $\varphi = 120°r$; (b), (e), (h) $j = 2$, $\varphi = 120°r$; (c), (f), (i) $j = 3$, no dependence on ψ. In graphs (a), (b), (d), (e), (g), and (h), curves 1, 2, 3, 4, 5, 6, and 7 were calculated for $\psi = 0°$, 15°, 30°, 45°, 60°, 75°, and 90°, respectively, and $r = 0$, 1, 2, 3.

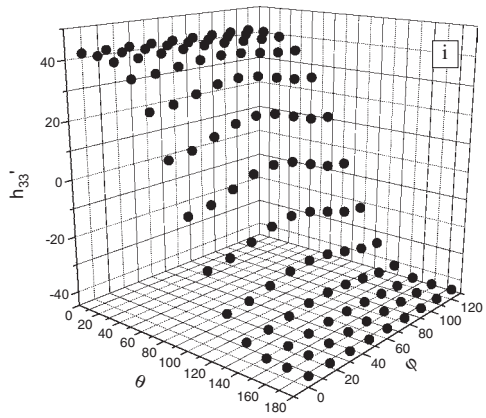

Figure 3. (Continued.)

into consideration in piezoelectric applications. For example, relations (6) and (7) show that the dependence of the piezoelectric coefficients d'_{3j} in the $3m$ class is similar to the orientation dependence determined for the single-domain ferroelectric SC in the $4mm$ class (e.g., $BaTiO_3$ or $PbTiO_3$) or for the poled ferroelectric ceramic (symmetry ∞mm). Furthermore, the similarity relationship is observed in periodicity on 90° and 60° as established in equalities (2), (3), and (6)–(8).

A similarity in configurations of d'_{3j} and g'_{3j} curves (compare, for example, figures 2(a) and 3(d) or figures 2(i) and 3(f)) as well as of e'_{3j} and h'_{3j} curves (compare, for example, figures 3(c) and (i)) is mainly explained by the passive role of dielectric constants ε'^{T}_{lm} and ε'^{S}_{lm}. These constants, being the components of the second-rank tensors, cannot considerably affect the orientation dependence of the piezoelectric coefficients, being the components of the third-rank tensors. In contrast to this, an effect of elastic moduli c'^{E}_{rt} or elastic compliances s'^{E}_{rt}, being the components of the fourth-rank tensors, results in considerable transformation of curves at transitions from d'_{3j} to e'_{3j} (compare, for example, figures 2(a) and 3(a) or figures 2(i) and 3(c)) or from g'_{3j} to h'_{3j} (compare, for example, figures 3(d) and (g) or figures 3(f) and (i)). In the last case, the piezoelectric coefficients $g'_{3j} = h'_{3f}s'^{D}_{fj}$ and $h'_{3j} = g'_{3f}c'^{D}_{fj}$ are connected through the elastic constants c'^{D}_{fj} or s'^{D}_{fj} which are measured at constant electric displacements [28]; however, this connection cannot result in considerable changes in the configuration of the curves shown in figure 3. Orientation behaviour of the electromechanical coupling factors k'_{3j} (figure 4) provides an additional argument on the passive role of the dielectric properties in forming the $k'_{3j}(\varphi, \psi, \theta)$ dependences. Comparing figures 2–4 at the corresponding fixed φ angles, we see that the transformation of curves $d'_{3j} \rightarrow g'_{3j} \rightarrow k'_{3j}$ is mainly explained by the orientation dependence of the elastic compliances $s'^{E}_{rt}(\varphi, \psi, \theta)$ of the single-domain SC.

3. Concentration dependences of electromechanical properties in the multidomain state

Now we consider two examples of the piezoelectric activity of multidomain PMN–0.33PT SCs. As is known from earlier papers [16, 22], multidomains are created in bulk SC samples when the poling direction is not along the spontaneous polarization vectors of the domains. In the case of the rhombohedral PMN–xPT SCs, it is assumed that the $(001)_c$ cut, poled along the $[001]_c$ direction in the perovskite axes OX°_{j}, contains 71° (109°) domains, being twin components. The orientations of the spontaneous polarization vectors $\mathbf{P_{si}}$ of these domains

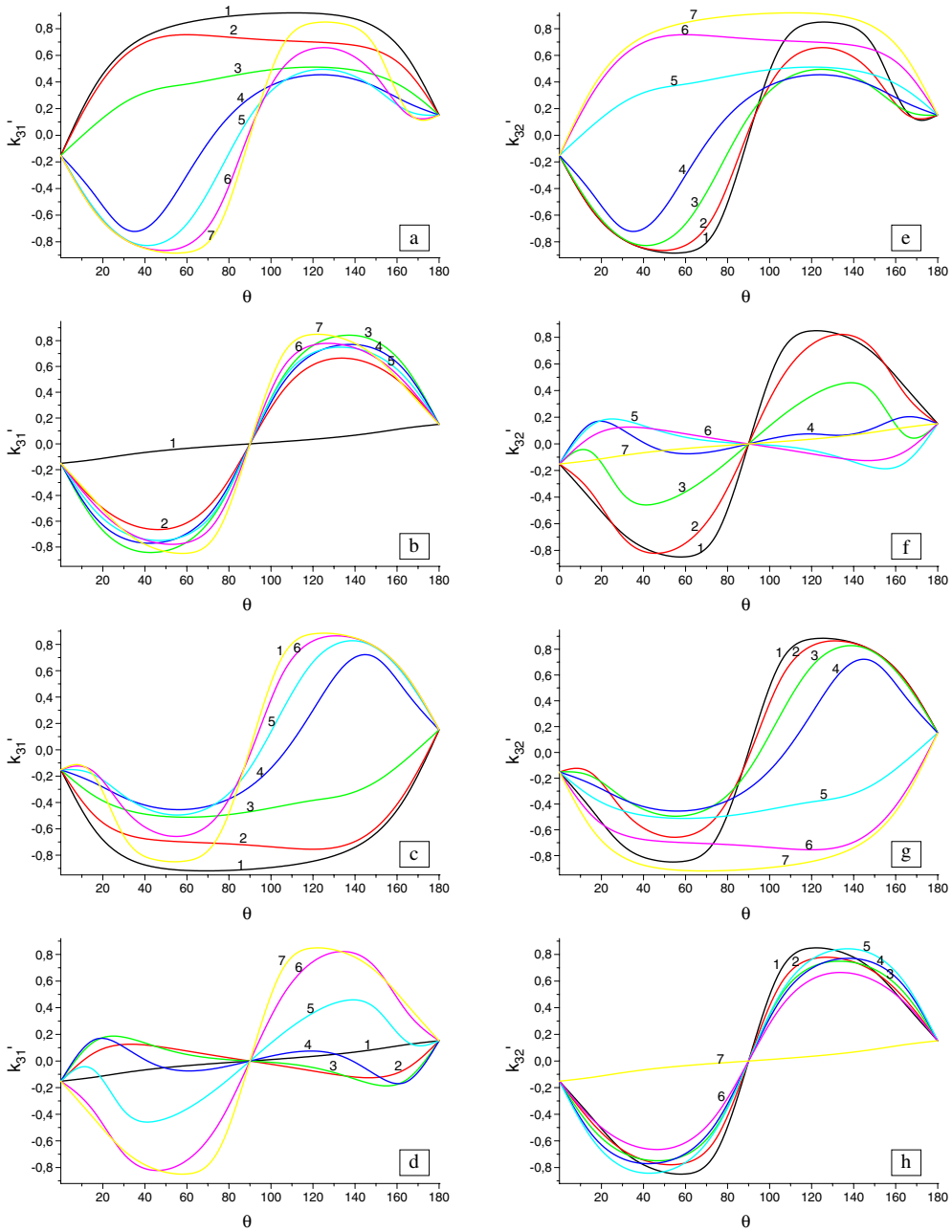

Figure 4. Electromechanical coupling factors $k'_{3j}(\varphi, \psi, \theta)$ (φ, ψ, and θ in degrees) calculated for the single-domain PMN–0.33PT SC. All further notations coincide with those given in the caption of figure 2.

are written in the coordinate system $(X_1^\circ X_2^\circ X_3^\circ)$ as follows: $\mathbf{P_{s1}}(P, P, P)$, $\mathbf{P_{s2}}(P, -P, P)$, $\mathbf{P_{s3}}(-P, -P, P)$, and $\mathbf{P_{s4}}(-P, P, P)$. The 71°(109°) domains are separated by $\{100\}_c$-type domain walls [2, 3, 19], this being permissible according to results of [29].

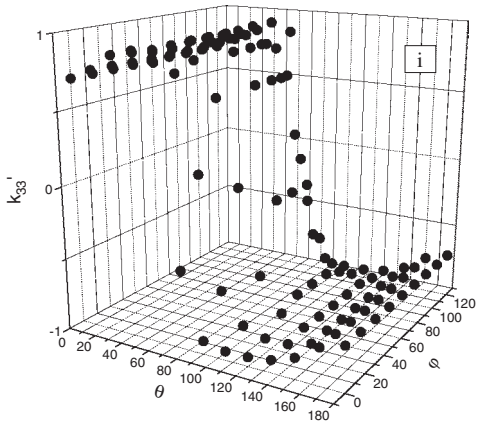

Figure 4. (Continued.)

3.1. Two domain types

It is assumed that the laminated domain structure in the SC sample is characterized by two domain types with the above-introduced vectors $\mathbf{P_{s1}}$ and $\mathbf{P_{s2}}$ and by the horizontal domain walls with normal vectors $\mathbf{n_i} \parallel [001]_c$. Volume concentrations of the domains with $\mathbf{P_{s1}}$ and $\mathbf{P_{s2}}$ equal h and $1 - h$, respectively. The electromechanical constants of the ith domain type are determined in the $(X_1^\circ X_2^\circ X_3^\circ)$ system in accordance with equations (1), where the rotation matrices are written in the form

$$\|\alpha\| = \begin{cases} \begin{pmatrix} 1/\sqrt{2} & -1/\sqrt{2} & 0 \\ 1/\sqrt{6} & 1/\sqrt{6} & -2/\sqrt{6} \\ 1/\sqrt{3} & 1/\sqrt{3} & 1/\sqrt{3} \end{pmatrix} & \text{for } i = 1 \\ \begin{pmatrix} 1/\sqrt{2} & 0 & -1/\sqrt{2} \\ 1/\sqrt{6} & 2/\sqrt{6} & 1/\sqrt{6} \\ 1/\sqrt{3} & -1/\sqrt{3} & 1/\sqrt{3} \end{pmatrix} & \text{for } i = 2. \end{cases}$$

The procedure of averaging the electromechanical constants of these two domain types is carried out by using the matrix approach developed in works [9–11]. Taking into account boundary conditions [8, 9, 27, 30] for electric and mechanical fields in adjacent domains, we calculated a full set of the effective elastic compliances $s_{rt}^{*\mathrm{E}}(h)$, piezoelectric coefficients $d_{fj}^{*}(h)$, and dielectric constants $\varepsilon_{lm}^{*\mathrm{T}}(h)$ of the multidomain SC in the range of $0 < h < 1$. Results of calculations of the piezoelectric coefficients $d_{3j}^{*}(h)$ and electromechanical coupling factors

$$k_{3j}^{*}(h) = d_{3j}^{*}(\varepsilon_{33}^{*\mathrm{T}} s_{jj}^{*\mathrm{E}})^{-1/2} \tag{10}$$

are shown in figure 5. It is important to note that minima of all the $|d_{3j}^{*}(h)|$ and $|k_{3j}^{*}(h)|$ functions occur at $h = 0.5$, i.e., at equal volume concentrations of the 71° (109°) domains. The same concentration dependence (figure 5) holds true for the above-mentioned laminated domain structure with $\mathbf{P_{s1}}$ (volume concentration h) and $\mathbf{P_{s4}}$ (volume concentration $1 - h$). The substitution of the first domain type by the fourth domain type does not affect either $d_{3j}^{*}(h)$ or $k_{3j}^{*}(h)$ due to symmetry features of this domain structure. This becomes clearer from the determination of the spontaneous polarization vector $\mathbf{P_{s,SC}}$ of the multidomain SC as a whole. In both the cases, i.e. for $\mathbf{P_{s,SC}} = \mathbf{P_{s1}}h + \mathbf{P_{s2}}(1 - h)$ or $\mathbf{P_{s,SC}} = \mathbf{P_{s1}}h + \mathbf{P_{s4}}(1 - h)$, only one component of the $\mathbf{P_{s,SC}}$ vector depends on the volume concentration h, and this component is

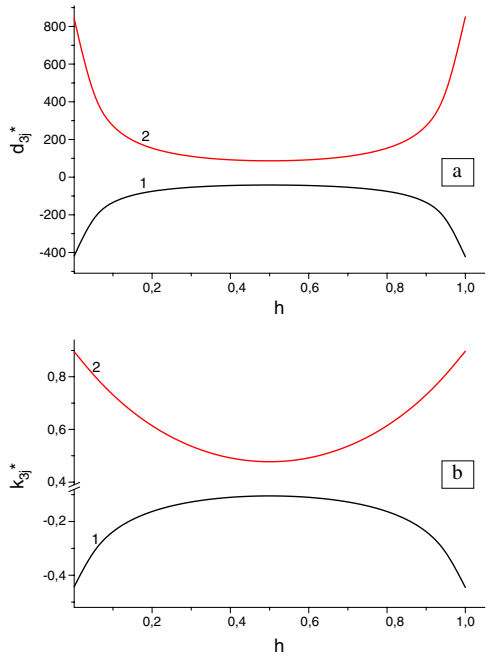

Figure 5. Effective piezoelectric coefficients $d^*_{3j}(h)$ (d^*_{3j} in pC N^{-1}, graph (a)) and electromechanical coupling factors $k^*_{3j}(h)$ (graph (b)) calculated for the multidomain PMN–0.33PT SC with spontaneous polarization vectors of domains $\mathbf{P_{s1}}$ and $\mathbf{P_{s2}}$. Curve 1 corresponds to $j = 1$ or 2, and curve 2 corresponds to $j = 3$.

related to one of the non-poling directions, OX_1° or OX_2°. If we consider a domain structure with $\mathbf{P_{s1}}$ and $\mathbf{P_{s3}}$, then the spontaneous polarization vector $\mathbf{P_{s,SC}} = \mathbf{P_{s1}}h + \mathbf{P_{s3}}(1-h)$ has two equal components, and these components are concerned with the non-poling directions OX_1° and OX_2°.

A similarity between the curves shown in figures 5(a) and (b) means that the piezoelectric coefficients $d^*_{3j}(h)$ considerably influence the concentration behaviour of the electromechanical coupling factors $k^*_{3j}(h)$ from equation (10). The low piezoelectric activity of the multidomain samples with $\mathbf{P_{s1}}$ and $\mathbf{P_{s2}}$ or with $\mathbf{P_{s1}}$ and $\mathbf{P_{s4}}$ along the OX_3° axis is accounted for a re-distribution of internal electric and mechanical stress fields and the clamping of non-180° domains in the presence of the domain walls with $\mathbf{n_i} \parallel [001]_c$.

3.2. Four domain types

Another interesting example of calculated concentration dependences of the effective electromechanical properties is associated with the domain structure shown in figure 6. It becomes clear from recent experimental papers [2, 6, 16, 19, 22], that such domain structures are often observed in the rhombohedral PMN–xPT and PZN–xPT SCs after poling along the OX_3° direction. In order to define the volume concentrations v_i of the adjacent domains we introduce two parameters, t and n (figure 6), and hereafter these concentrations are written as follows: $v_1 = tn$, $v_2 = t(1-n)$, $v_3 = (1-t)(1-n)$, and $v_4 = (1-t)n$. The effective electromechanical properties of the multidomain SC are calculated on the basis of a two-step averaging procedure described in paper [30]. Calculated concentration dependences $d^*_{3j}(t,n)$ and $k^*_{3j}(t,n)$, which characterize the piezoelectric activity and electromechanical coupling

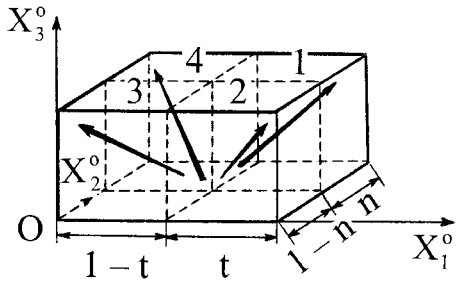

Figure 6. Schematic arrangement of 71° (109°) domains in the rhombohedral SC of PMN–xPT type. Spontaneous polarization vectors $\mathbf{P_{si}}$ ($i = 1, \ldots, 4$) of the four domain types are indicated by arrows. $(100)_c$ and $(010)_c$, domain walls separating different domain types. $(X_1^\circ X_2^\circ X_3^\circ)$, coordinate system with axes parallel to the perovskite unit-cell vectors.

along the poling axis OX_3°, are graphically represented in figure 7. As in the early-considered case of two domains (see section 3.1), the present domain structure (figure 6) provides decreasing both $|d^*_{3j}(t,n)|$ and $|k^*_{3j}(t,n)|$ at $t \to 0.5$ and/or $n \to 0.5$. A simple comparison of dependences $d^*_{33}(t,n)$ (figure 7(c)) and $k^*_{33}(t,n)$ (figure 7(d)) points out that the elastic compliance $s^{*\mathrm{E}}_{33}(t,n)$ and dielectric constant $\varepsilon^{*\mathrm{T}}_{33}(t,n)$ slightly influence electromechanical coupling (see equation (10)) in the multidomain state. Hence, the piezoelectric coefficient $d^*_{33}(t,n)$ plays the main role in forming this electromechanical coupling as the case of the SC with two domain types considered in section 3.1. However, the piezoelectric coefficient $d^*_{33}(t,n)$ (figure 7(c)) decreases in a fairly narrow range in comparison with $d^*_{33}(h)$ (see curve 2 in figure 5(a)) calculated for the SC with two domain types. In our opinion, such a difference in the concentration dependences is accounted for by the orientation of the domain walls in the bulk sample: a less considerable decrease is observed in the absence of the $(001)_c$ domain walls (figure 6), i.e., in the multidomain SC with the walls separating the domains along the non-poling directions OX_1° and OX_2° only.

The low piezoelectric activity of the multidomain SCs considered in sections 3.1 and 3.2 is associated with the intrinsic contribution from the non-180° domain structures to the piezoelectric coefficients $d^*_{3j,\mathrm{exp}}$ of real SCs. According to the known room-temperature data [15] on the PMN–0.33PT SC poled along the $[001]_c$ axis ($4mm$ symmetry), the effective values are $d^*_{31,\mathrm{exp}} = -1330$ pC N^{-1} and $d^*_{33,\mathrm{exp}} = 2820$ pC N^{-1} with the presence of the four 71° (109°) domain types (figure 6) with equal volume concentrations. The significant discrepancy between the calculated value of $d^*_{33}(0.5, 0.5) \approx 300$ pC N^{-1} and the above-given experimental $d^*_{33,\mathrm{exp}}$ value is in good agreement with one of the conclusions of work [5], and could be caused, probably, by inducing the intermediate monoclinic phase[2] near the morphotropic phase boundary, by the non-180° domain coexistence [32], or by displacements of interfaces [33, 34] separating two coexisting phases under the external electric field $\mathbf{E} \parallel [001]_c$. Unfortunately, the lack of experimental work on interconnections between the electromechanical properties of the single-domain and multidomain PMN–xPT SCs prevents us from comparing different results with due attention. However, some results of the present study are important for a comparative analysis of the known data on the related PZN–xPT SCs near the morphotropic phase boundary.

[2] It should be mentioned that Kisi *et al* [31] recently reported new results on the piezoelectric effect in the related PZN–xPT SCs near the morphotropic phase boundary. It has been shown that the field-induced rhombohedral–monoclinic phase transition is neither sufficient nor necessary to understand the large piezoelectric response, and significant softening of some elastic constants at the morphotropic phase boundary is ultimately responsible for the large $d^*_{3j,\mathrm{exp}}$ values.

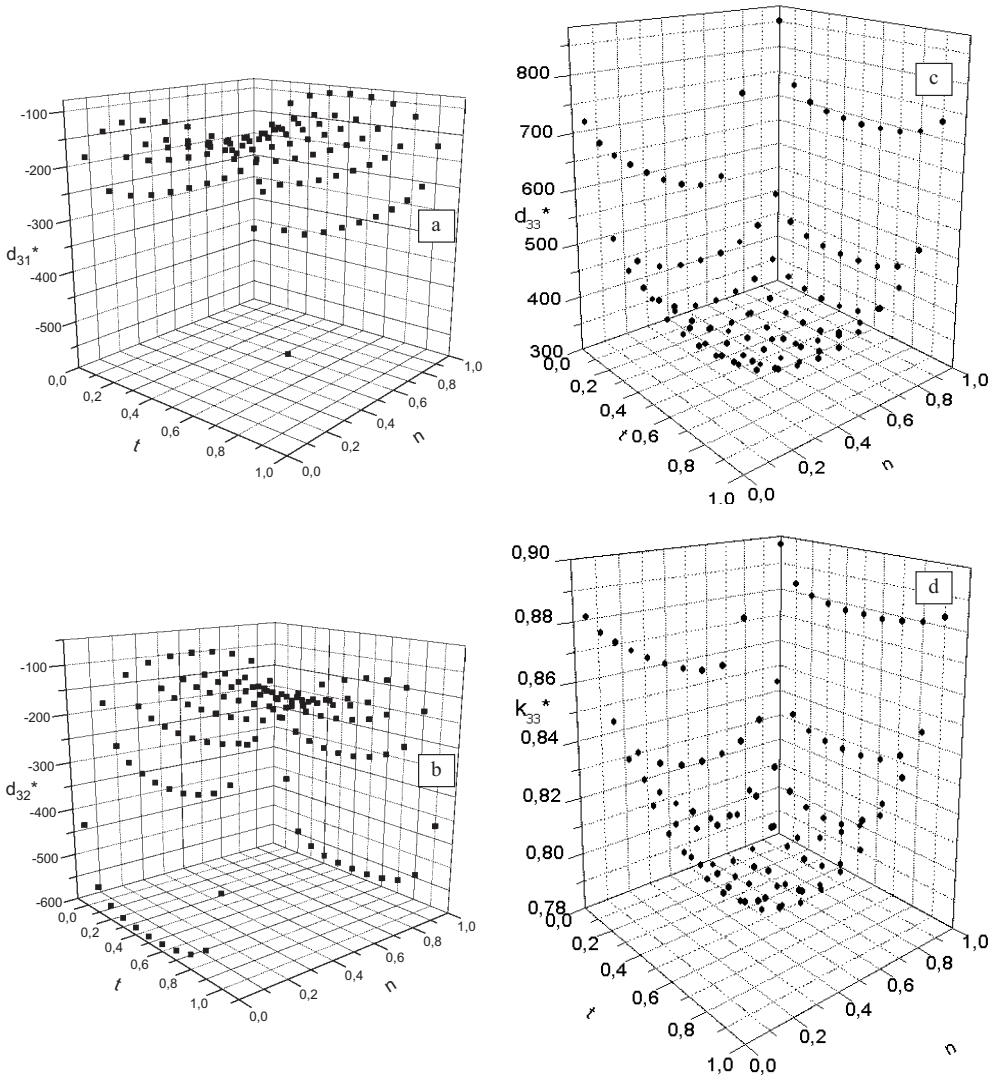

Figure 7. Effective piezoelectric coefficients $d_{3j}^*(t, n)$ (d_{3j}^* in pC N^{-1}, graphs (a)–(c)) and electromechanical coupling factor $k_{33}^*(t, n)$ (graph (d)) which were calculated for the PMN–0.33PT SC with the domain arrangement shown in figure 6.

On the one hand, Dammak *et al* [32] very recently experimentally determined the complete set of the intrinsic piezoelectric coefficients $d_{3j,\mathrm{exp}}$ in the quasi-single-domain monoclinic PZN–0.09PT SC and described an effect of domain coexistence on the piezoelectric coefficients d_{3j}^* of multidomain samples. The engineered domain structure, containing four non-180° domain types in the monoclinic phase, is analogous to that shown in figure 6. The poling field $\mathbf{E} \parallel [001]_\mathrm{c}$ applied to such samples induces an additional (or extrinsic) internal mechanical stress field. The spontaneous polarization vectors of these domains tend to tilt toward the **E** direction, but this tilting is restricted by the system of the $(100)_\mathrm{c}$ and $(010)_\mathrm{c}$ domain walls like those shown in figure 6. As a result, values of the piezoelectric coefficients $d_{3j,\mathrm{exp}}^*$ measured on the $(001)_\mathrm{c}$ cuts of the above-mentioned PZN–0.09PT SCs are more than twice the calculated d_{3j}^* values.

On the other hand, our previous evaluations [33] made for the multidomain PZN–xPT SC near the morphotropic phase boundary ($x = 0.08$–0.09, single-domain $3m$ phase) show that the contribution Δd^*_{33} from the displacement of the interface with the normal vector $\mathbf{n_i} \parallel \mathbf{E} \parallel [001]_c$ accounts for 50–90% of the experimental $d^*_{33,\mathrm{exp}}$ value. Furthermore, the displacement of the like interface in the same PZN–xPT SC upon the rhombohedral–monoclinic phase transition induced by the electric field $\mathbf{E} \parallel [001]_c$ results in the considerable (up to 90%) contribution Δd^*_{33} to $d^*_{33,\mathrm{exp}}$, and the calculated $\Delta d^*_{33}(E)$ and $d^*_{33,\mathrm{exp}}(E)$ curves are characterized by similarity over a wide electric field range [34].

In our opinion, the above-mentioned circumstances are to be regarded as good arguments for the important role of the interfaces in the analogous case, as the very high piezoelectric activity is achieved in the multidomain PMN–xPT SCs with the rhombohedral structure. The more detailed study of the effect of the non-180° domain structure on the piezoelectric activity of the PMN–xPT SCs and especially of the extrinsic contribution to the piezoelectric coefficients $d^*_{3j,\mathrm{exp}}$ may be a subject of further experimental work.

4. Conclusion

In this paper, important examples of the orientation and concentration dependences of the piezoelectric coefficients and electromechanical coupling factors have been considered for the rhombohedral $3m$ phase of PMN–0.33PT SCs. In the single-domain state, non-monotonic orientation dependences of the piezoelectric coefficients d'_{3j}, e'_{3j}, g'_{3j}, and h'_{3j} and electromechanical coupling factors k'_{3j} have been determined for $j = 1, 2, 3$ and analysed in terms of Euler angles. Different variants of periodicity of these orientation dependences have been revealed and explained by taking into account unit-cell symmetry features. It has been shown that the second-rank and fourth-rank tensors linking four types of the piezoelectric coefficients, being the components of the third-rank tensors, affect changes in their orientation dependences (figures 2 and 3) in different ways. The last result is believed to be true for single-domain states in different symmetry classes allowing the piezoelectric effect.

In the multidomain state, two variants of the non-180° domain structures have been studied, and their effective piezoelectric coefficients d^*_{3j} and electromechanical coupling factors k^*_{3j} have been calculated at various volume concentrations of several domain types. It has been shown that the corresponding SCs are characterized by $\min |d^*_{3j}(h)|$ and $\min |k^*_{3j}(h)|$ (figures 5 and 7) in the 'most symmetrical' cases of the domain arrangement, i.e., as equal volume concentrations of the 71°(109°) domains separated by the $\{100\}_c$-type walls are attained and the domain-wall displacement is neglected. Our calculation data on the multidomain SCs correspond to the intrinsic contribution from the non-180° domain structures to effective electromechanical constants of SCs.

Finally, the results of this work will provide the necessary input for interpretation of the unusual electromechanical response of the single-and multidomain relaxor-based SCs near the morphotropic phase boundary. These results can be a stimulus for a further study of various complicated domain (twin) structures and engineered domain structures and their role in forming the effective physical properties of modern piezoelectric and ferroelectric materials.

Acknowledgments

The author would like to thank Dr D Damjanovic (Switzerland) and Dr M Kamlah (Germany) for their constant interest in the research problem and discussions as well as Mme D Stern (Germany) for technical assistance. The author is grateful to Dr C R Bowen (United Kingdom)

for careful reading of the amended version. Financial support by the Research Centre Karlsruhe (Germany) during the stay of the author at the Research Institute IMF II of the above-mentioned centre is gratefully acknowledged.

References

[1] Kuwata J, Uchino K and Nomura S 1981 *Ferroelectrics* **37** 579
Kuwata J, Uchino K and Nomura S 1982 *Japan. J. Appl. Phys.* **21** 1298
[2] Park S-E and Shrout T R 1997 *J. Appl. Phys.* **82** 1804
Park S-E and Shrout T R 1997 *Mater. Res. Innov.* **1** 20
[3] Erhart J and Cao W 1999 *J. Appl. Phys.* **86** 1073
[4] Zhang R, Jiang B and Cao W 2003 *Appl. Phys. Lett.* **82** 3737
[5] Damjanovic D, Budimir M, Davis M and Setter N 2003 *Appl. Phys. Lett.* **83** 527
Damjanovic D, Budimir M, Davis M and Setter N 2003 *Appl. Phys. Lett.* **83** 2490 (erratum)
[6] Liu T and Lynch C S 2003 *Acta Mater.* **51** 407
[7] Feng Z, Luo H, Guo Y, He T and Xu H 2003 *Solid State Commun.* **126** 347
[8] Turik A V 1970 *Fiz. Tverd. Tela* **12** 892 (in Russian)
Turik A V 1970 *Sov. Phys.—Solid State* **12** 688 (Engl. Transl.)
[9] Akcakaya E and Farnell G W 1988 *J. Appl. Phys.* **64** 4469
[10] Topolov V Yu 1995 *J. Phys.: Condens. Matter* **7** 7405
[11] Topolov V Yu and Turik A V 1998 *J. Phys.: Condens. Matter* **10** 451
[12] Ye Z-G and Dong M 2000 *J. Appl. Phys.* **87** 2312
[13] Xu G, Luo H, Xu H and Yin Z 2001 *Phys. Rev.* B **64** 020102
[14] Iwata M, Araki T, Maeda M, Suzuki I, Ohwa H, Yasuda N, Orihara H and Ishibashi Y 2002 *Japan. J. Appl. Phys.* **41** 7003
[15] Zhang R, Zhiang B and Cao W 2001 *J. Appl. Phys.* **90** 3471
[16] Yin J and Cao W 2002 *J. Appl. Phys.* **92** 444
[17] Ren W, Liu S-F and Mukherjee B K 2002 *Appl. Phys. Lett.* **80** 3174
[18] Nosek J and Erhart J 2003 *Microelectron. Eng.* **66** 733
[19] Wada S, Park S-E, Cross L E and Shrout T R 1999 *Ferroelectrics* **221** 147
[20] Baba-Kishi K Z, Pang G K H, Choy C L, Chan H L W, Luo H, Yin Q and Yin Z 2001 *Ferroelectrics* **253** 55
[21] Ogawa T and Numamoto Y 2002 *Japan. J. Appl. Phys.* 1 **41** 7108
[22] Yin J, Jiang B and Cao W 2000 *IEEE Trans. Ultrason. Ferroelectr. Freq. Control* **47** 285
Yin J, Jiang B and Cao W 1999 *Proc. SPIE Conf. on Ultrasonic Transducer Engineering (San Diego, CA, 1999)*; *Proc. SPIE* **3664** 239
[23] Numamoto Y, Yamaguchi Y, Ogawa T, Matsushita M and Tachi Y 2002 *Key Eng. Mater.* **228/229** 9
[24] Zhang R, Jiang W, Jiang B and Cao W 2002 *Fundamental Physics of Ferroelectrics* (*AIP Conf. Proc.*) ed R E Cohen (Melville, NJ: American Institute of Physics) p 188
[25] Cao H and Luo H 2002 *Ferroelectrics* **274** 309
[26] Zhang R, Jiang B and Cao W 2003 *Appl. Phys. Lett.* **82** 787
[27] Nye J F 1957 *Physical Properties of Crystals* (Oxford: Clarendon)
Ikeda T 1990 *Fundamentals of Piezoelectricity* (Oxford: Oxford University Press)
[28] Zheludev I S 1968 *Physics of Crystalline Dielectrics* (Moscow: Nauka) (in Russian)
Zheludev I S 1971 *Physics of Crystalline Dielectrics* (New York: Plenum)
[29] Fousek J and Janovec V 1969 *J. Appl. Phys.* **40** 135
[30] Glushanin S V and Topolov V Yu 2001 *J. Phys. D: Appl. Phys.* **34** 2518
[31] Kisi E H, Piltz R O, Forrester J S and Howard C J 2003 *J. Phys.: Condens. Matter* **15** 3631
[32] Dammak H, Renault A-É, Gaucher P, Thi M P and Calvarin G 2003 *Japan. J. Appl. Phys.* 1 **42** 6477
[33] Topolov V Yu and Turik A V 2001 *Phys. Solid State* **43** 1117
[34] Topolov V Yu and Turik A V 2002 *Phys. Solid State* **44** 1355